Nuclear Engineering and Technology 52 (2020) 1495–1502

Contents lists available at ScienceDirect

Nuclear Engineering and Technology

journal homepage: www.elsevier.com/locate/net

Original Article

A method of X-ray source spectrum estimation from transmission measurements based on compressed sensing

Bin Liu*, Hongrun Yang, Huanwen Lv, Lan Li, Xilong Gao, Jianping Zhu, Futing Jing

Science and Technology on Reactor System Design Technology Laboratory, Nuclear Power Institute of China, Chengdu, 610213, China

ARTICLE INFO

Article history:
Received 28 July 2019
Received in revised form
23 November 2019
Accepted 3 December 2019
Available online 4 December 2019

Keywords:
X-ray source spectrum estimation
Transmission measurements
Compressed sensing and sparse representation

ABSTRACT

A new method of X-ray source spectrum estimation based on compressed sensing is proposed in this paper. The algorithm K-SVD is applied for sparse representation. Nonnegative constraints are added by modifying the L_1 reconstruction algorithm proposed by Rosset and Zhu. The estimation method is demonstrated on simulated spectra typical of mammography and CT. X-ray spectra are simulated with the Monte Carlo code Geant4. The proposed method is successfully applied to highly ill conditioned and under determined estimation problems with a good performance of suppressing noises. Results with acceptable accuracies (MSE < 5%) can be obtained with 10% Gaussian white noises added to the simulated experimental data. The biggest difference between the proposed method and the existing methods is that multiple prior knowledge of X-ray spectra can be included in one dictionary, which is meaningful for obtaining the true X-ray spectrum from the measurements.

1. Introduction

Knowledge of X-ray spectrum is very important for determining the radiation dose, reducing beam-hardening artifacts, and dual-energy material decomposition analysis of diagnostic X-ray imaging and CT [1,2]. It is difficult to measure spectrum from the X-ray tube directly due to the high source intensity. The transmission method, which involves a phantom of known dimensions and compositions, is widely used for X-ray spectrum determination for its simplicity and adaptability to a large energy range of X-ray [3,4]. The penetration rate p of polychromatic X-rays through the material with thickness L can be formulized as [4],

$$p \pm p_{Noise} = \frac{I}{I_0} = \int_{E_{\min}}^{E_{\max}} D(E)s(E)e^{-\int_L \mu(E,r)dl}dE = \int_{E_{\min}}^{E_{\max}} W(E)e^{-\int_L \mu(E,r)dl}dE \quad (1)$$

where p_{Noise} is the noise added to p in the experimental filed; I_0 and I are incident and transmitted photon intensities; $W(E)$ denotes the overall spectrum, which combines the X-ray source spectrum $s(E)$ and the detector response $D(E)$.

Eq. (1) can be converted into a linear system by discretization,

$$p_q \pm \varepsilon_q = \sum_{p=1}^{N} A_{p,q} w_p, \quad q = 1, \ldots, M$$
$$A_{pq} = \exp\left(- \int_L \mu_q(E_p, r)dl \right) \quad (2)$$

where ε_q is the noise term of the experimental data; M is the total number of measurements; N is the number of samplings of the spectrum; A is the measurement matrix calculated from the linear attenuation coefficients and thickness of the phantom, and w_p is the spectrum sampling.

To make it easier to discuss, Eq. (2) is written in the matrix form,

$$P \pm \varepsilon = AW \quad (3)$$

where P is a $M \times 1$ vector consisting of the transmission data; ε is a $M \times 1$ vector consisting of the noise term of the experimental data; A is the measurement matrix with dimension of $M \times N$; and W is a $N \times 1$ vector consisting of the spectrum sampling.

Normally, M is of the order of dozens and N is of the order of

* Corresponding author.
E-mail address: liubin871204@126.com (B. Liu).

https://doi.org/10.1016/j.net.2019.12.004

hundreds, which makes the X-ray estimation problem stated in Eq. (3) is not only ill conditioned, but also under-determined. Some numerical methods have been proposed and applied to this problem. One of them is the EM (expectation-maximization) method. The EM method minimizes the Kullbeck-Liebler distance to the transmission data. The positivity of the solution is automatically enforced and the prior information is often used as the initial guess [5]. The current methods, including the EM method, focus mainly on the illness condition of the problem. The prior information is often used as the initial guess to start the algorithm. Therefore, only single prior information can be used in one estimation. However, there might be multiple guesses or predictions of the spectrum to be estimated. These guesses or predictions can all be used as prior information. Therefore, it is quite necessary to develop new estimation method which not only focuses on the illness condition of the problem, but also on new ways of using the prior information.

Compressed sensing (CS) theory, proposed by Donoho, T. Tao and Candes, is a new method to reconstruct signals from significantly fewer samplings. The CS theory is considered as a breakthrough of the Nyquist-Shannon sampling theory and is widely used in areas of medical imaging, analog-digital conversion, computational biology and other aspects [6–8]. The CS theory claims that the unique solution can be obtained for the under determined problem on some certain conditions.

In this paper, CS theory is introduced to solve the under determined problem stated in Eq. (3). Part 2 presents the model, introducing CS theory to the X-ray spectrum estimation problem. Part 3 applies the method discussed in Part 2 to simulated transmission measurements. X-ray spectra with an energy range of mammography imaging and energy range of CT are estimated respectively. Performances of the method are evaluated, including the dependence on the prior information, noise suppression ability, and the ability of using multiple prior information.

2. The estimation method based on compressed sensing

2.1. Estimation model

As is discussed in part 1, the X-ray spectrum estimation problem stated in Eq. (3) is under determined so there is no unique solution. However, according to the CS theory, the unique solution can be obtained as long as the X-ray spectrum W is sparse (usually not) or can be presented sparsely by a linear combination of a complete basis, shown in Eq. (4),

$$W = \Psi\beta \tag{4}$$

where Ψ is a sparse basis matrix, which is also called the dictionary. The representative stated in Eq. (4) is called a kind of sparse representation, through which β is sparse and the problem has the unique solution.

With the appropriate dictionary Ψ and substituting Eq. (4) into Eq. (3), then we have,

$$P \pm \varepsilon = X\beta \tag{5}$$

where X equals $A\Psi$. Then the unique solution can be obtained by solving Eq. (5), which is equivalent to,

$$\widehat{\beta} = \underset{\beta}{\operatorname{argmin}} \|\beta\|_0 \quad s.t. \quad \|P - X\beta\|_2^2 \le \varepsilon \tag{6}$$

where $\|\cdot\|_0$ denotes the L_0 norm, which represents the number of non-zero entries.

Solving Eq. (6) is called reconstruction. Finally, the X-ray spectrum can be obtained with appropriate β, shown by Eq. (7),

$$\widehat{W} = \Psi\widehat{\beta} \tag{7}$$

2.2. Sparse representation of X-ray spectrum

As discussed, the unique solution can be obtained as long as W can be represented sparsely. So choice of the dictionary is very important. Fourier basis, discrete cosine basis, and discrete wavelet basis are widely used for sparse representation in image processing and other aspects for their mathematical completeness and easy to implement [9]. However, these methods are not adaptive and not suitable for spectra estimation. Therefore, the dictionary based on learning is considered. Given a set of training samples $Y = \{y_i\}_{i=1}^N$, the dictionary D is searching for the best representation, as is shown in Eq. (8),

$$\min_{D,\alpha} \|Y - D\alpha\|_2^2 s.t. \forall i \|\alpha_i\|_0 \le t \tag{8}$$

where α is sparse coefficient and t is the sparsity, namely the number of nonzero entries of α.

To obtain dictionary D requires two processes: sparse coding and dictionary update. Sparse coding is the process of computing the representation coefficients based on the given samples and the dictionary D. This process, commonly referred to as “atom decomposition”, requires solving the following equation,

$$\min_{\alpha_i} \|y_i - D\alpha_i\|_2^2 s.t. \|\alpha_i\|_0 \le t \tag{9}$$

The dictionary update process is as follows: assume both α and D are fixed. Consider d_k (one column in D) and the corresponding coefficient α_k (the kth row in α), the penalty term can be written as Eq. (10),

$$\begin{aligned} \|Y - D\alpha\|_2^2 &= \left\| Y - \sum_{j=1}^{K} d_j\alpha_j \right\|_2^2 \\ &= \left\| \left(Y - \sum_{j\neq k} d_j\alpha_j \right) - d_k\alpha_k \right\|_2^2 \\ &= \|E_k - d_k\alpha_k\|_2^2 \end{aligned} \tag{10}$$

The K-SVD algorithm, which is a generalization of K-means (developed by Michal Aharon et al.) [10], is applied to update the learning dictionary in this paper. The K-SVD algorithm uses orthogonal matching pursuit (OMP) algorithm, which is a greedy algorithm that selects the dictionary atoms sequentially, involving computation of inner products between the signal and dictionary columns, deploying least squares solvers for sparse coding [11], and SVD decomposition of E_k is used to update the dictionary. For the SVD decomposition finds the closest rank-1 matrix that approximates E_k, which can minimizes Eq. (10) effectively. Restrictions on matrix Y, D, and α_k are applied for enforcing the sparsity constraints.

2.3. The reconstruction algorithm

Direct solution of Eq. (6) proves to be NP-hard. A common solution is convex relaxation which relaxes the L_0 norm to the L_1 norm, shown in Eq. (11),

$$\min \|\beta\|_1 \quad s.t. \quad \|P - X\beta\|_2^2 \le \varepsilon \tag{11}$$

Eq. (11) can be written as Lagrange multiplier,

$$\widehat{\beta}(\lambda) = \underset{\beta}{\operatorname{argmin}} \ \|P - X\beta\|_2^2 + \lambda\|\beta\|_1 \tag{12}$$

Eq. (12) is the famous Lasso (least absolute shrinkage and selection operator) model, which consists of a least square estimate and a L_1 norm penalty. The parameter λ denotes the penalty factor which can be deemed as the weight between cost function and the penalty term.

A number of algorithms have been proposed for lasso solution. The algorithm used in this paper is mainly based on the Matlab tool spaSM [12], which is based on the method proposed by Rosset and Zhu [13]. The algorithm uses Taylor expansions of the norm equations of the minimization problem stated in Eq. (12) to get $\nabla\beta$, shown in Eq. (13),

$$\nabla\widehat{\beta}(\lambda) = -\left(2X_{\mathscr{A}}^{\mathrm{T}}X_{\mathscr{A}}\right)^{-1} \cdot \operatorname{sign}(\widehat{\beta}_{\mathscr{A}}(\lambda)) \tag{13}$$

where $\mathscr{A}$ is called the active set, denoting indices in β corresponding to non-zero elements.

Eq. (12) is rewritten with expanded set of β values like $\beta_j = \beta_j^+ + \beta_j^-$, where $\beta_j^+ \geq 0$ and $\beta_j^- \geq 0$, $\forall j$. Considering the Karush-Kuhn-Tucker conditions of the optimization problem, the properties of the distance γ can be obtained, shown in Eq. (14) and Eq. (15) [12],

$$j \in \mathscr{A} \rightarrow \mathscr{T}: \quad \widehat{\beta}_j^{(k)} + \gamma \ \nabla\widehat{\beta}_j^{(k)} = 0, \quad j \in \mathscr{A} \tag{14}$$

$$\begin{aligned} j \in \mathscr{T} \rightarrow \mathscr{A}: \ & \left|\left(\nabla L\left(\widehat{\beta}^{(k)} + \gamma \ \nabla\widehat{\beta}^{(k)}\right)\right)_i\right| \\ & = \left|\left(\nabla L\left(\widehat{\beta}^{(k)} + \gamma \ \nabla\widehat{\beta}^{(k)}\right)\right)_j\right|, \quad j \in \mathscr{A}, \ i \in \mathscr{T} \end{aligned} \tag{15}$$

where $\mathscr{T}$ is called the inactive set and denotes the complement of $\mathscr{A}$. Eq. (14) defines the distances $\{\gamma\}$ at which active variables hit zero and join $\mathscr{T}$. Eq. (15) defines the distances at which inactive variables join $\mathscr{A}$. The smallest value $\gamma_{\min}$ is where the next event will happen.

With $\nabla\beta$ obtained in Eq. (13) and γ obtained in Eq. (14) and Eq. (15), the coefficients can be updated by,

$$\widehat{\beta}^{(k+1)} = \widehat{\beta}^{(k)} + \gamma_{\min}\nabla\widehat{\beta}^{(k)} \tag{16}$$

The algorithm proposed by Rosset and Zhu can solve the lasso problem with high efficiency and accuracy, as well as has the ability to suppress the noises. The only drawback is that it does not enforce the non-negativity. So the method is modified in this paper. The modification is simple, by which the negative entries of W in Eq. (7) are set to be zeros to make sure entries of the final estimated X-ray spectra (stated in Eq. (7)) are non-negative. The flow chart of the modified LASSO algorithm is illustrated in Fig. 1. Steps 13 to 16 are the modified steps.

It is obvious to see from Eq. (12) that the accuracy of the reconstruction is highly depended on the value of λ. The larger the value of λ is, the sparser coefficient vector β is; while the smaller the value of λ is, the more convex the reconstruction process is, which leads to higher accuracy of the reconstruction. There are some criteria for trading off the sparsity and the accuracy, such as the Akaike's Information Criterion (AIC), Bayesian Information Criterion (BIC) and so on. In this paper, the AIC criterion is applied.

The AIC of the kth iteration can be defined as [14],

1: Initialize $\beta^{(0)} = \mathbf{0}$, $\mathcal{A} = \arg\max_j \left|x_j^{\mathrm{T}} y\right|$, $\nabla\hat{\beta}_{\mathcal{A}}^{(0)} = -\operatorname{sign}\left(x_{\mathcal{A}}^{\mathrm{T}} y\right)$, $\nabla\hat{\beta}_{\mathcal{T}}^{(0)} = 0$, $k = 0$.
2: while $\mathcal{T} \neq \varnothing$ do
3: $\gamma_j = \min_{j \in \mathcal{A}}^{+} - \beta_j^{(k)} \big/ \nabla\beta_j^{(k)}$
4: $\gamma_i = \min_{i \in \mathcal{A}}^{+} \left\{ \dfrac{\left(x_i + x_j\right)^{\mathrm{T}}\left(y - X\hat{\beta}^{(k)}\right)}{\left(x_i + x_j\right)^{\mathrm{T}}\left(X\nabla\hat{\beta}^{(k)}\right)}, \dfrac{\left(x_i - x_j\right)^{\mathrm{T}}\left(y - X\hat{\beta}^{(k)}\right)}{\left(x_i - x_j\right)^{\mathrm{T}}\left(X\nabla\hat{\beta}^{(k)}\right)} \right\}$
5: $\gamma = \min\left\{\gamma_j, \gamma_i\right\}$
6: if $\gamma = \gamma_j$ then
7: Move j from $\mathcal{A}$ to $\mathcal{T}$
8: else
9: Move i from $\mathcal{T}$ to $\mathcal{A}$
10: end if
11: $\hat{\beta}^{(k+1)} = \hat{\beta}^{(k)} + \gamma\hat{\beta}^{(k)}$
12: $\nabla\hat{\beta}^{(k+1)} = -\left(2X_{\mathcal{A}}^{\mathrm{T}}X_{\mathcal{A}}\right)^{-1} \cdot \operatorname{sign}\left(\hat{\beta}_{\mathcal{A}}^{(k+1)}\right)$
13: $W^{(k+1)} = D\hat{\beta}^{(k+1)}$
14: if $W^{(k+1)}(p) < 0, (p = 1, \ldots, N)$ then
15: $W^{(k+1)}(p) = 0$
16: end
17: $k = k + 1$
18: end while
19: Output the series of coefficients $B = \left[\beta^{(0)} \ldots \beta^{(k)}\right]$.

Fig. 1. LASSO algorithm modified with non-negative modification.

$$AIC^{(k)} = \left\|P - X\beta^{(k)}\right\|^2 + 2\sigma^2 df^{(k)} \tag{17}$$

where $df^{(k)}$ is the degree of freedom, which is given by the number of non-zero elements of β; and σ^2 represents the residual variance which can be defined as,

$$\sigma^2 = \frac{1}{n}\|P - X^+P\|^2 \tag{18}$$

where X^+ is the Moore-Penrose pseudo-inverse of X.

3. Simulation studies

3.1. Monte Carlo simulation of the source spectrum

X-ray spectra with an energy range of mammographic imaging and energy range of CT are both studied in this section. In mammographic imaging, the X-ray energies are generally on the lower end of the diagnostic imaging range, so the simulation considers X-rays generated by Mo (molybdenum) source and filtered by half a millimeter of aluminum; while in CT application, the subjects often have higher X-ray attenuation, therefore the simulation considers X-rays generated by W (tungsten) source and filtered by 1 cm of aluminum.

The X-ray source spectra used in this paper are all simulated with the Monte Carlo toolkit Geant4 [15–16]. The "G4UAtomicDeexcitation" class is implemented for simulating the production of X-rays by electron source, and the standard EM (Electro-Magnetic) package is used for photo-electric effect and Compton scattering of X-rays. Threshold cuts of 0 μm is applied for both electrons and X-rays, corresponding to energy cuts of 990 eV in molybdenum, aluminum, and tungsten. The simulation results of X-rays generated by Mo source with accelerating voltage of 25 kV and X-rays generated by W source with accelerating voltage of 140 kV are shown in Fig. 2. The peaks in the spectrum are characteristic lines of Mo (17.443 keV and 19.633 keV, shown in Fig. 2a), and the characteristic lines of W (58.5 keV and 61.7 keV, shown in Fig. 2b).

The energy range of X-ray photons for mammographic imaging is from 3.5 keV to 25 keV, and the energy range of X-ray photons for

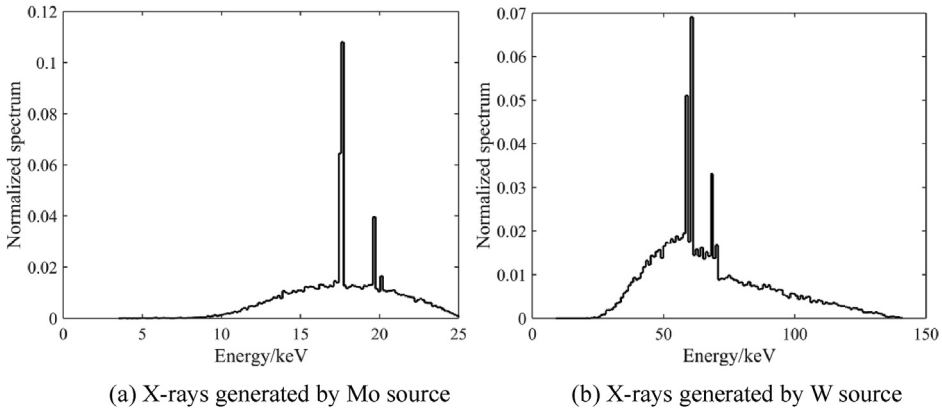

Fig. 2. X-ray source spectra obtained with Geant4 simulation.

CT is from 9 keV to 141 keV. There are 140 energy bins for both mammographic imaging and CT. The X-ray spectra shown in Fig. 2 are used as the test spectra to be estimated in this paper.

3.2. Design of the measurement matrix

The measurement matrix is obtained through two step-wedge phantoms. Materials for the phantoms are aluminum (Al) and carbon (C) for their different attenuation levels. Description of the step phantoms is listed in Table 1.

As is discussed above, for both the mammographic imaging and CT problem, there are 140 energy bins of X-ray spectrum and the number of equations is 40. The problem is highly under determined and ill conditioned. The condition number of the system matrix A are in a magnitude of 10^{21} (for mammographic imaging) and 10^{24} (for CT). The following part of this paper is the application of the estimation method discussed in Part 2 to X-ray estimation of mammographic imaging and CT.

3.3. The estimation results

3.3.1. Results of the mammographic spectrum

As is discussed above, the X-ray spectrum estimation problem is an under determined and there must be prior information to get

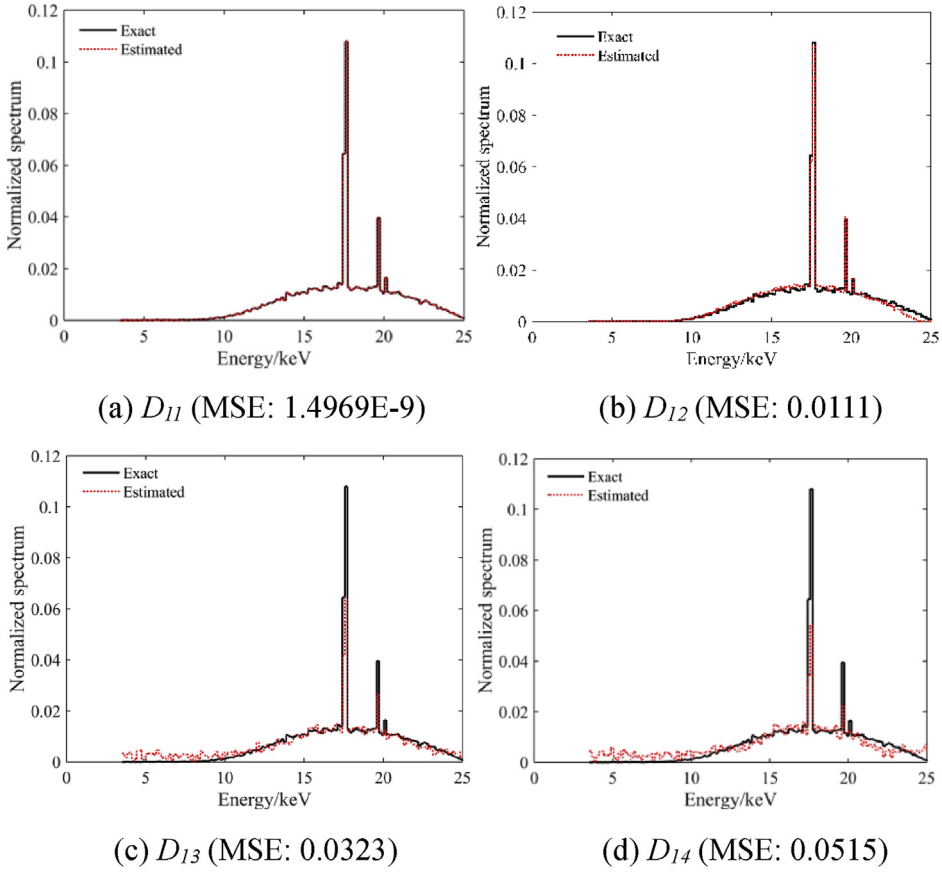

Fig. 3. Estimated results with different prior spectra.

Table 1
Technical description of step phantoms.

Phantom material	Mass density (g/cm^3)	Number of steps	Minimum thickness (cm)	Maximum thickness (cm)
Aluminum	2.7	20	0.127	2.54
Carbon	1.6825	20	0.212	4.24

the desired solution. To study the dependence of the estimation accuracy on the prior information, 4 dictionaries D_{11}, D_{12}, D_{13}, and D_{14} are tested respectively. The corresponding training spectra are X-ray spectra simulated with the accelerating voltages of 25 kV, 24 kV, 23 kV and 22 kV. The estimation results are illustrated in Fig. 3. The accuracy of the estimation is evaluated by MSE (Mean Square Error), which is described in Eq. (19),

$$\mathrm{MSE} = \sqrt{\sum_{i=1}^{N}\left(W_i^{\mathrm{Estimated}} - W_i^{\mathrm{Exact}}\right)^2} \tag{19}$$

The X-ray spectrum can be estimated almost exactly while it can be represented sparsely enough, shown in Fig. 3 (a). The accuracy drops while the prior spectrum deviates from the spectrum to be estimated. However, estimated results with acceptable accuracies can be obtained with sufficient prior information.

Normally, the transmission data are always contaminated by the noises of the experimental ground, which causes difficulty of the estimation. To study the noise suppression ability of the method, estimation is carried out with 1%, 3%, 5%, and 10% Gaussian white noises added to the transmission data. Dictionary D_{12} is used for sparse representation. The estimated results are shown in Fig. 4. While the accuracy drops as the level of noise grows, the estimation method has a strong ability to suppress noises. The X-ray spectrum can still be estimated with an acceptable accuracy (MSE<0.05) with 10% Gaussian white noises added, shown in Fig. 4 (d).

The biggest difference between the estimation method proposed in this paper and the existing estimation methods is the way using prior information. The current methods use the prior information as the initial guess to start the algorithm. While the method proposed in this paper uses the prior information as the training samples for sparse representation, which allows use of multiple prior information. To verify this, estimation is carried out and the estimated results are shown in Fig. 5. The dictionary D_{15} is used for sparse representation. Dictionary D_{15} is obtained by the K-SVD algorithm illustrated in Part 2 with X-ray spectra simulated with the accelerating voltages of 25 kV, 24 kV, 23 kV, 22 kV, 20 kV and 18 kV respectively. The estimation is carried out with 3% Gaussian white noises added to the transmission data. The test spectra are X-ray spectra simulated with the accelerating voltages of 24 kV, 23 kV, 22 kV and 20 kV respectively.

As is shown in Fig. 5, estimated results with acceptable accuracies can be obtained for their prior information are included in the training matrix. This is quite meaningful for multiple prior information can be included on one dictionary for sparse representation.

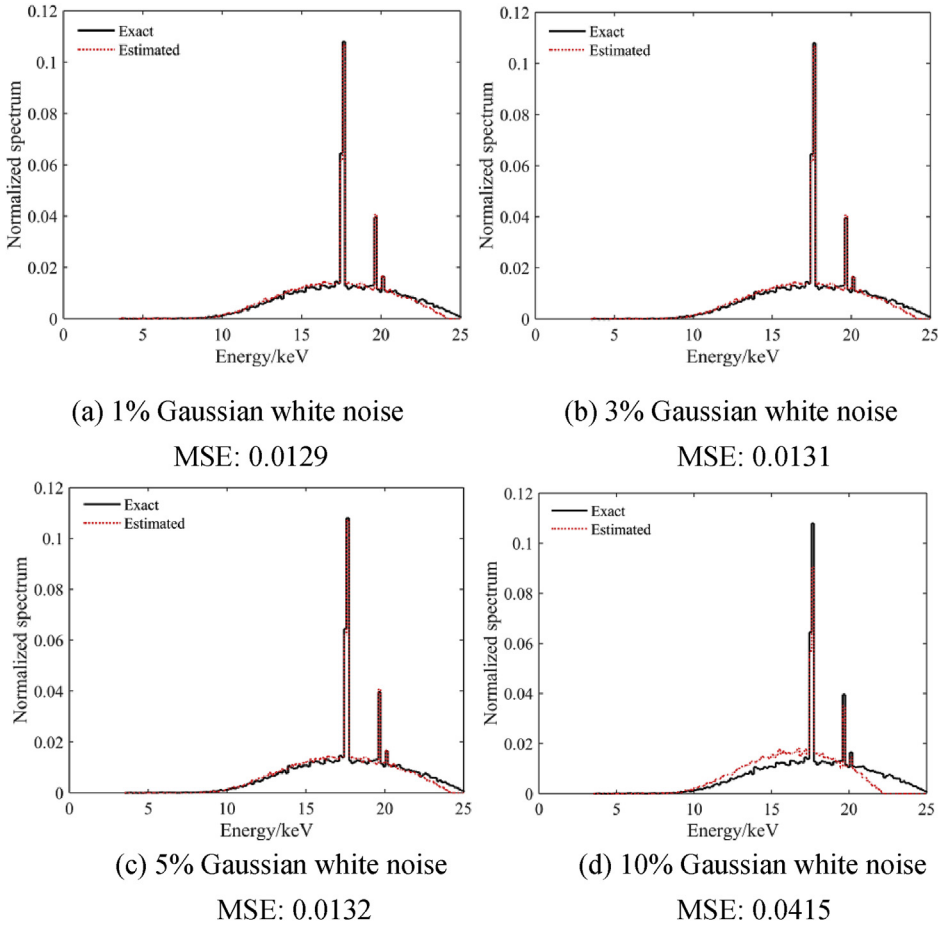

Fig. 4. Estimated results with different levels of noises.

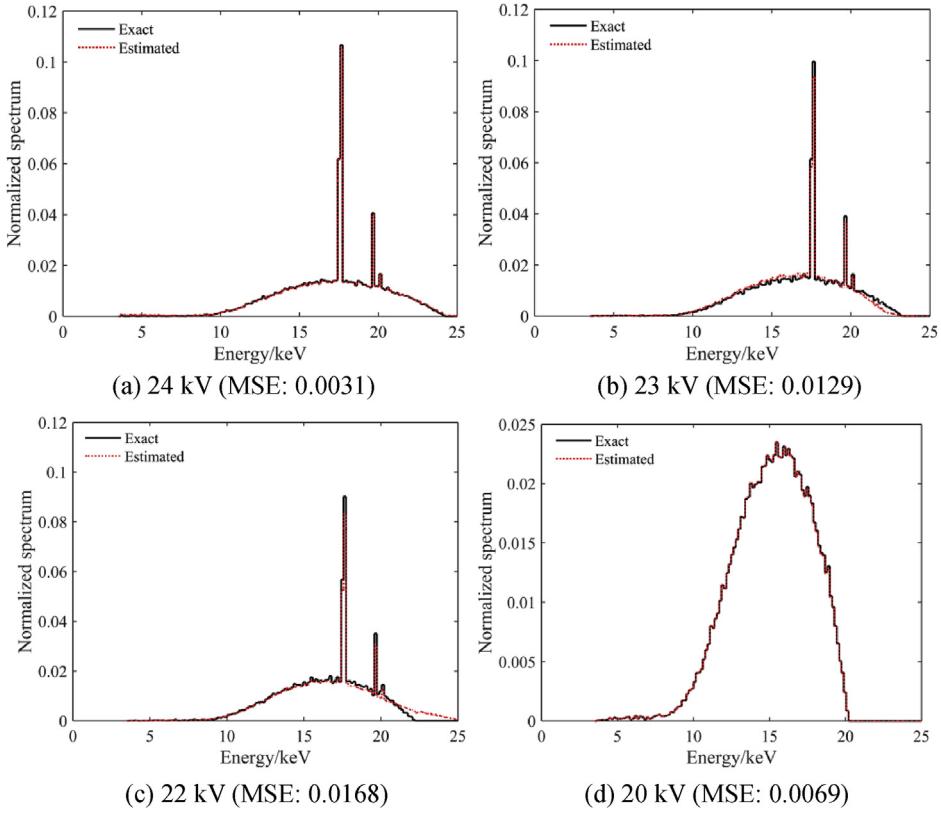

Fig. 5. Estimated results with multiple prior spectra.

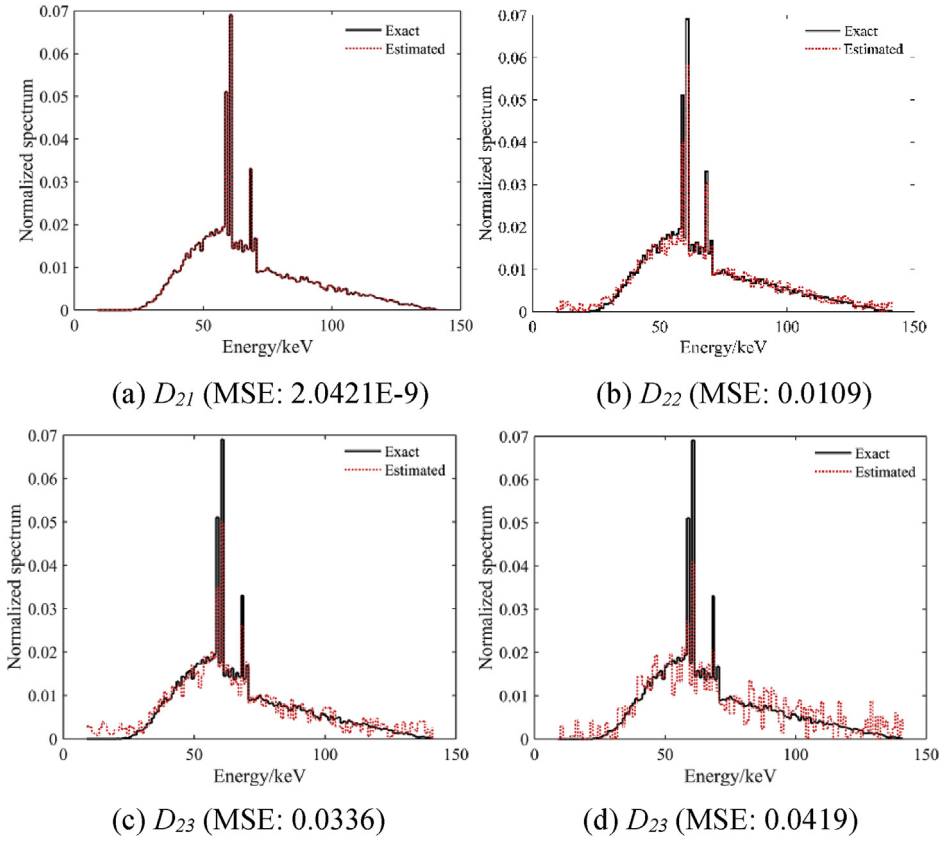

Fig. 6. Estimated results with different prior spectra.

3.3.2. Results of the CT spectrum

As is discussed in the former part, the estimation method discussed in Part 2 can be successfully applied to X-ray spectrum estimation for mammographic imaging application. However, the X-ray spectrum in CT application is quite different both in spectrum shape and energy range of X-rays. To study the adaptability of the estimation method, the X-ray spectrum of CT application is tested for estimation. Firstly, 4 dictionaries D_{21}, D_{22}, D_{23}, and D_{24} are tested respectively. The corresponding training spectra are X-ray spectra simulated with the accelerating voltages of 140 kV, 130 kV, 120 kV and 110 kV. The estimated results are shown in Fig. 6.

Similarly, Gaussian white noises with levels of 1%, 3%, 5% and 10% are added to the transmission data. The estimated results are shown in Fig. 7. Dictionary D_{22} is used for sparse representation. Noises can be well suppressed. Acceptable accuracy can be obtained (MSE<0.05) with 10% Gaussian white noises added, shown in Fig. 7 (d).

Dictionary D_{25} with multiple prior information is tested. The training spectra are X-ray spectra simulated with the accelerating voltages of 140 kV, 135 kV, 130 kV, 120 kV, 110 kV and 100 kV. X-ray spectra simulated with the accelerating voltages of 130 kV, 120 kV, 110 kV and 100 kV are tested. 3% Gaussian noises are added to the transmission data. The estimated results are shown in Fig. 8.

As is shown in Fig. 8, estimated results with acceptable accuracies can be obtained for their prior information are included in the training matrix. Like the estimation for X-ray spectrum of mammographic imaging, X-ray spectrum of CT can also be estimated with acceptable accuracies with the estimation method proposed in Part 2.

4. Discussion and conclusion

A new estimation method based on compressed sensing for X-ray spectrum estimation is proposed in this paper. The prior spectra are used as training samples of the dictionary for sparse representation. K-SVD algorithm is applied for dictionary learning. Convex relaxation is used for reconstruction by transforming L_0 norm problem into the Lasso problem. An algorithm proposed by Rosset and Zhu is applied for solving Lasso, non-negative constraints are enforced by the modification of the Rosset and Zhu's algorithm. The estimation method is demonstrated on simulated spectra typical of mammography and CT, which are obtained with the Monte Carlo code Geant4.

As to the highly ill conditioned and under determined problem of X-ray spectrum estimation, results with better accuracies are obtained with prior knowledge. The method has a good ability of suppressing noises. Results with acceptable accuracies (MSE < 5%) can be obtained with 1% Gaussian white noises added to the simulated experimental data, both for X-ray spectra of mammographic imaging and CT.

The biggest difference between the method proposed in this paper and the existing methods is the use of the prior knowledge. As to the existing methods, prior knowledge is used as the initial guess of the algorithm; while the method proposed in this paper uses the prior knowledge as the training samples for sparse representation. The advantage of this method is that multiple prior knowledge can be included in one dictionary for sparse representation, which is meaningful for obtaining the true X-ray spectrum from the measurements.

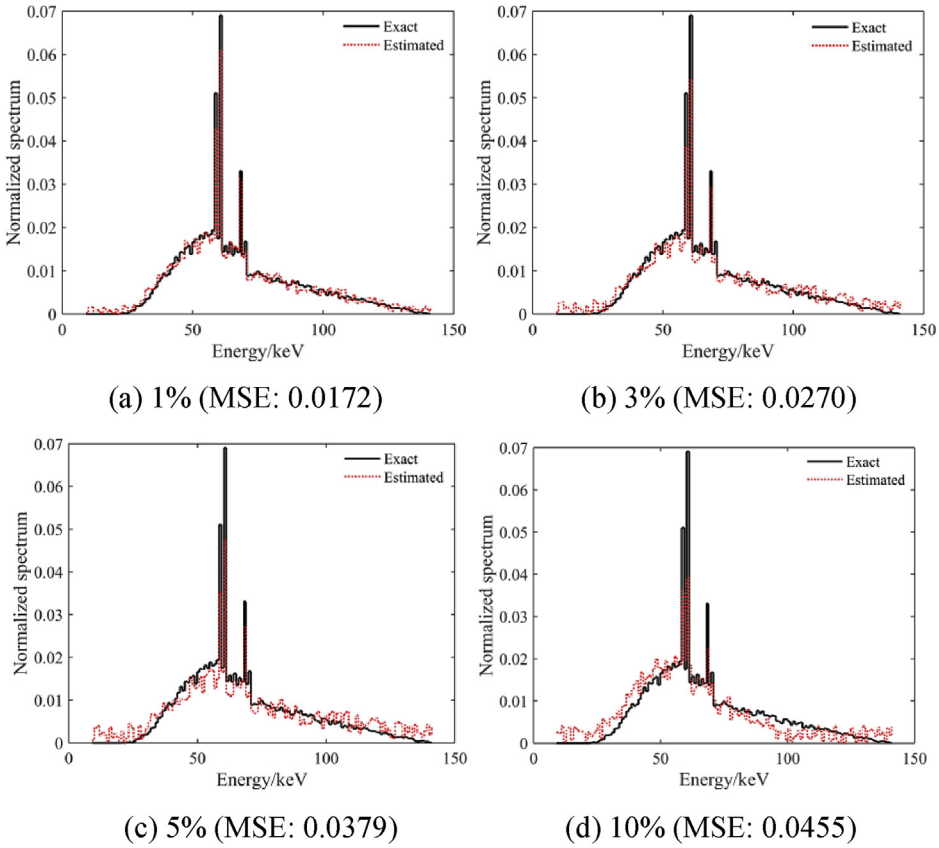

Fig. 7. Estimated results with different levels of noises.

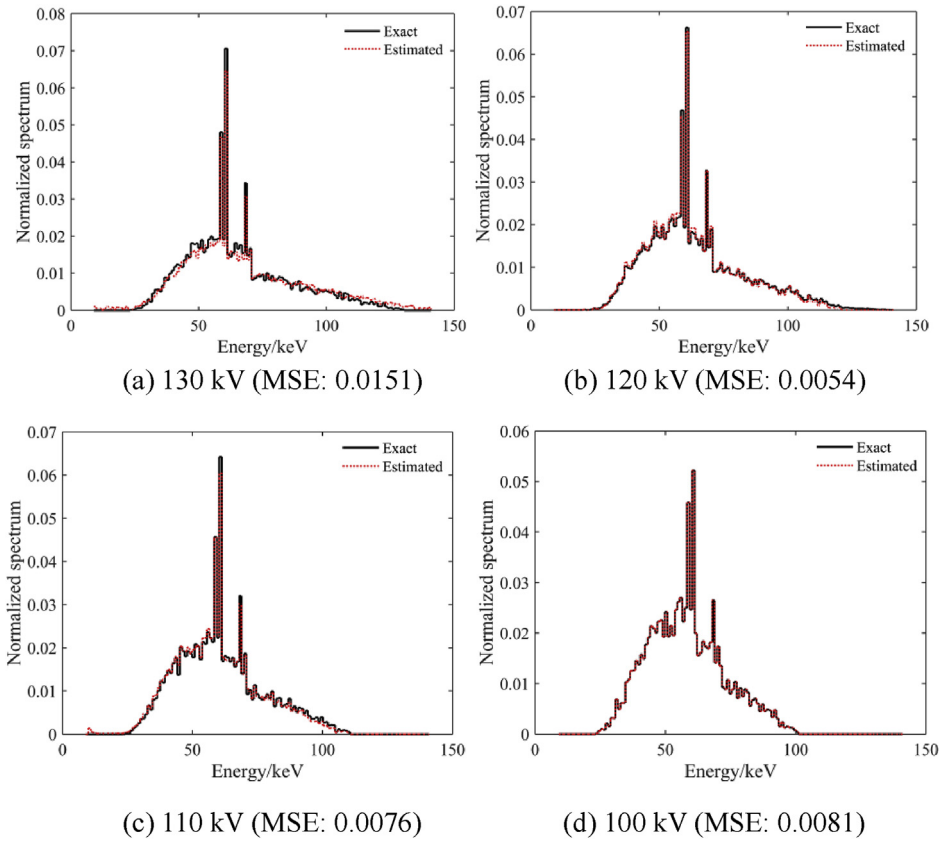

Fig. 8. Estimated results with multiple prior spectra.

Declaration of competing interest

There is no conflict of interest.

Appendix A. Supplementary data

Supplementary data to this article can be found online at https://doi.org/10.1016/j.net.2019.12.004.

References

[1] P. Engler, W.D. Friedman, Review of dual-energy computed tomography techniques, Mater. Eval. 48 (1990) 623–629.
[2] B.J. Heismann, J. Leppet, K. Stierstorfer, Density and atomic number measurements with spectral X-ray attenuation method, J. Appl. Phys. 94 (3) (2003) 2073–2079.
[3] Li Zhang, Guowei Zhang, Zhiqiang Chen, et al., X-ray estimation from transmission measurements using the expectation maximization method, in: IEEE Nuclear Science Symposium Conference Record, 2007.
[4] Xinhui Duan, Jia Wang, Lifeng Yu, et al., CT scanner X-ray spectrum estimation from transmission measurements, Med. Phys. 38 (2) (2011) 993–997.
[5] Emil Y. Sidky, Lifeng Yu, Xiaochuan Pan, et al., A robust method of X-ray source spectrum estimation from transmission measurements: demonstrated on computer simulated, scatter-free transmission data, J. Appl. Phys. 97 (2005), 1247011-12470111.
[6] E. Candes, J. Romberg, T. Tao, Stable signal recovery from incomplete and inaccurate measurement, Commun. Pure Appl. Math. 59 (8) (2010) 1207–1223.
[7] M. Lustin, D. Donoho, J.M. Pauly, Sparse MRI: the application of compressed sensing for rapid MR imaging, Magn. Reson. Med. 58 (6) (2010) 1182–1195.
[8] M.A. Davenport, J.N. Laska, J.R. Treichler, et al., The Procs and Cons of compressive sensing for wideband signal acquisition: noise folding versus dynamic range, IEEE Trans. Signal Process. 60 (2011) 4628–4642.
[9] Simon Foucart, Holger Rauhut, A Mathematical Introduction to Compressed Sensing, Springer, New York, 2013.
[10] Michal Aharon, Michael Elad, Alfred Bruckstein, K-SVD: an algorithm for designing overcomplete dictionaries for sparse representation, IEEE Trans. Signal Process. 11 (54) (2006) 4311–4322.
[11] Y.C. Pati, R. Rezaiifar, P.S. Krishnaprasad, Orthogonal matching pursuit: recursive function approximation with applications to wavelet decomposition, in: Proceedings of 27th Asilomar Conference on Signals, Systems and Computers, 1993.
[12] Sjostrand Karl, et al., SpaSM: a MATLAB took box for sparse statistical Modeling, J. Stat. Softw. 84 (10) (2018) 1–37.
[13] Saharon Rosset, Ji Zhu, Picewise linear regularized solution paths, Ann. Stat. 35 (3) (2007) 1012–1030.
[14] Efron Bradley, Trevor Hatie, Iain Johnstone, Robert Tibshirani, Least angle regression, Ann. Stat. 32 (2) (2004) 407–499.
[15] S. Agostinelli, et al., Geant4: a simulation toolkit, Nucl. Instrum. Methods Phys. Res. 506 (3) (2003) 250–303.
[16] J. Allison, et al., Geant4 developments and applications, IEEE Trans. Nucl. Sci. 53 (1) (2006) 1412–1419.